Heat Transfer in a Hot Stamping Process: A Review

R Muvunzi[a], DM Dimitrov[a], S Matope[a], TM Harms[b]

Received 21 September 2016, in revised form 31 July 2017 and accepted 21 September 2017

Abstract: Heat transfer rate during the hot stamping process affects the resultant quality and production rate of the process. This is because the ability of the tool to transfer heat from the blank affects the resultant tensile strength, temperature distribution and cooling time of the formed part. Research efforts have been made on the design of cooling systems that are aimed towards improving the cooling effectiveness of the blanks thereby improving the quality characteristics of the formed parts. The cooling rate is governed by the interfacial heat transfer coefficient (IHTC). A proper design of hot stamping tools requires knowledge of the heat transfer modes during the hot stamping process. It is important to gain an understanding of the heat transfer scenarios during the process to seek opportunities to reduce the cooling time and improve the quality of parts. The purpose of this article is to review the heat transfer phases during the hot stamping cycle and propose a model for the heat loss by the blank during the process. A review of the models that can be utilized to determine IHTC is presented.

Additional keywords: Die design, hot sheet metal forming, heat balance, heat transfer model, cooling layout design

Nomenclature

Roman

A	Surface area [m^2]
a	Distance between cooling channels [mm]
b	Distance from surface to cooling channel centre [mm]
Bi	Biot number ($Bi = \frac{hL}{k}$)
c	Specific heat capacity [J/kgK]
d	Cooling channel diameter [mm]
E	Latent heat energy [J/kg]
f	Shape factor
F	Force [N]
Gr	Grashof number ($Gr = \frac{L^3\rho^2 g\Delta T\beta}{\mu^2}$)
g	Air gap thickness [mm]
H	Hardness [N/m^2]
h	Convection heat transfer coefficient [W/m^{2}K]
L	Length scale of blank [m]
k	Thermal conductivity [W/mK]
l	Length of cooling channel [m]
m	Mass [kg]
n	Number of cooling channels
Nu	Nusselt number $[Nu = hD/k]$
Pr	Prandtl Number $[Pr = \mu c/k]$
P	Pressure [MPa]
$\dot{Q}$	Heat transfer rate [W]
R	Interfacial heat transfer coefficient [W/m^{2}K]
r	Radius of cooling channel [mm]
s	Slope of surface roughness [µm]
T	Temperature [K]
t	Time [s]
U	Martensitic transformation fraction [%]
V	Volume of blank [m^3]
v	Velocity [m/s]
$\dot{W}$	Rate of work done [W]
w	Centre distance of cooling channels [mm]
x	Thermal conduction direction [mm]
y	Thickness [mm]
Z	Distance cooling channel centre to die surface [mm]

Greek

α	Fraction of plastic work done converted into heat
β	Coefficient of volume expansion of fluid [K^{-1}]
δ	Error function
ε	Emissivity of blank
ϵ	Strain rate [s^{-1}]
λ	Material constant [K^{-1}]
µ	Viscosity [kg/sm]
ɲ	Coefficient of friction
η	Standard deviation of surface roughness (rad)
ρ	Density of blank [kg/m^3]
σ	Stefan Boltzmann constant [Wm^{-2}K^{-4}]
τ	Stress [N/m^2]
Φ	Conductance [W/m^{2}K]

Subscripts

av	Average
a	Ambient
b	Blank
bd	Surface area of blank exposed to die
bp	Surface area of blank exposed to punch
bot	Bottom
conv	Convection
con	Conduction
cw	Cooling channel wall
d	Die
fac	Floor and ceiling surfaces in the plant
form	Forming phase
g	Air gap conductance
i	Initial
in	Inlet
ms	Martensitic start
out	Outlet
p	Punch
plac	Placement phase

a. Department of Industrial Engineering, Stellenbosch University, rmuvunzi@sun.ac.za
b. SAIMechE Fellow, Department of Mechanical and Mechatronic Engineering, Stellenbosch University, tmh@sun.ac.za.

rad	Radiation
s	Solid conductivity
top	Top
total	Total
tran	Transfer phase
w	Coolant in channels (water)

1 Introduction

The global goals of the automotive industry include the increase in safety and the reduction of vehicle weight [1]. This has led to the application of the hot stamping process in the production of crash relevant components with complex shapes, high strength (up to 1500 MPa) and reduced weight [2]. According to Karbasian and Tekkaya [3], hot stamping processes can be classified as direct and indirect hot stamping. Direct hot stamping involves firstly heating a blank (thin metal sheet) to a temperature between 900 and 950 K and transferring it to a press for forming and quenching. This results in the formed blank having a martensitic structure with high strength (1500 MPa). In indirect hot stamping, the blank is firstly pre-cold formed before it is formed and quenched in a press [3]. One of the crucial goals in research involving hot sheet metal forming technology includes the reduction in cycle time and this is highly influenced by the cooling time of the blank in a closed tool during the forming and quenching stage [4]. An analysis of the hot stamping process showed that at least 30 % of the cycle time involves cooling and holding the blank in a closed tool [5]. The forming and quenching stage also affects the resultant tensile strength and temperature distribution of the formed part [6]. This is because hot stamping is a thermo-mechanical process whereby the cooling rate affects the resultant microstructural properties of the formed part [7,8]. To improve the quality characteristics of the formed part (tensile strength), it is necessary to increase the heat transfer rate between the blank and tool. This can be established by improving the cooling system of the tools. Research efforts have been made to develop models for designing and optimizing the cooling system of the tools in order to increase the cooling rate and achieve a more uniform temperature distribution of the formed part surfaces [6,9,10,11,12]. The developed models and optimization methods are useful in determining the cooling system structural parameters which maximizes heat transfer. However, some of the models are computationally intensive and not applicable for tools with complex geometry. Another strategy involves the use of tool materials with high thermal conductivity [13,14,15]. On the other hand, some of the materials are costly and still in their development stages.

Heat transfer between blank and tool can be measured based on the interfacial heat transfer coefficient (IHTC). Currently, there is no proper equipment dedicated to characterize the interfacial heat transfer coefficient because of the complexity of the hot stamping process [16]. Current research has focused on developing models for determining the IHTC and related parameters during hot stamping [7,17,18,19,20,21,22]. There is need to gain an understanding of the heat transfer modes during the hot stamping process in order to seek opportunities for reducing the cycle time and improving quality. This paper aims to propose a basis for the heat transfer model during the hot stamping process. The paper firstly presents an analysis of heat transfer during the process stages based on theory and literature study. This includes a review of the current research that has been done for the determination of IHTC. This is followed by a discussion and a proposed model which governs the overall heat transfer for the stamping cycle.

2 Heat transfer during the hot stamping process stages

The hot stamping process can be grouped into four stages. These stages include austenitization of the blank to 950 K in a furnace, transfer of the blank to the forming tool, forming and quenching in a closed tool[1] as shown in figure 1.

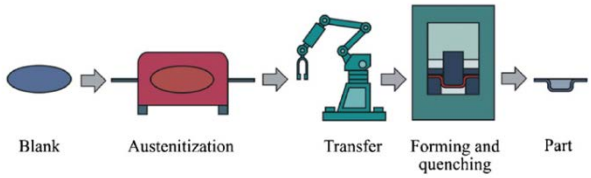

Figure 1 Direct hot stamping process [3]

To study the heat transfer from the blank during the process, it is necessary to analyse the stages in which heat is lost from the blank. It is assumed that the temperature across the blank is uniform because of the small thickness of blank (0.6-3 mm). Hence the rate of heat loss from the blank $\dot{Q}(t)$ can generally be expressed by equation 1 below.

$$\dot{Q}(t) = mc_b \frac{dT_b}{dt} \quad (1)$$

During the hot stamping process, the blank loses heat when it is transferred from the austenitization furnace to the forming tool ($\dot{Q}_{tran}$), when it is placed on the forming tool ($\dot{Q}_{plac}$) and when it is in contact with the forming tool during the forming and quenching phase ($\dot{Q}_{form}$). The heat lost by the blank during the above-mentioned stages ($\dot{Q}_{total}$) (the integral of equation 1), is considered as negative since heat is released from the blank. This can be expressed mathematically as shown in equation 2.

$$\dot{Q}_{total} = -\dot{Q}_{tran} - \dot{Q}_{plac} - \dot{Q}_{form} \quad (2)$$

The following section gives an analysis of the transfer, placement and forming stages.

2.1 Transfer Stage

During transfer from furnace to the stamping tool, the blank loses heat by radiation and convection to the surrounding air at atmospheric temperature [7,23]. Hence heat loss from the blank per given time is in the form of convective heat Q_{conv_1} and radiative heat Q_{rad_1} as shown in equation 3.

$$\dot{Q}_{tran} = \dot{Q}_{conv_1} + \dot{Q}_{rad_1} \quad (3)$$

It is assumed that the hot blank is transferred from the furnace to the forming tool in its horizontal position. However, this depends on the set up of a given industrial process. In order to determine the convective heat transfer during the transfer phase, the blank can be treated as a flat plate which loses heat on both sides by convection to ambient air [6,23,24] as shown in figure 2.

A small Biot number (Bi <<1) is assumed for the blank because of its small thickness (0.6-3mm), high thermal conductivity (32 W/mK) and large surface area to volume ratio which translates to a low characteristic length [23,25].

Furthermore, other authors from literature have also confirmed a small Biot number for the blank [17,26]. Based on this notion, the blank is considered to have uniform temperature during the transfer stage. The Biot number can be expressed using equation 4.

$$Bi = \frac{hL}{k} \tag{4}$$

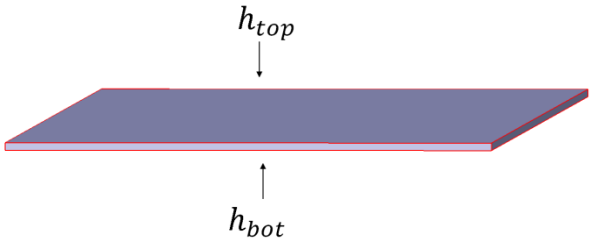

Figure 2 Heat loss of blank at the top and bottom surfaces

It can also be assumed that the heat lost on the edges of the blank is negligible due to the small thickness [7]. According to the process requirements, the blank must be transferred to the forming tool soon after release from the furnace [27]. The effect of natural convection must be considered depending on the set up of the process. If fast material handling devices such as robotic arms are used to rapidly transfer the blank to the furnace, the effect of natural convection may be neglected or be replaced by forced convection consideration. On the other hand if the blank is left for some time before the forming stage, it is necessary to include the effect of natural convection arising. To re-examine these effects preference is given to include the effect of natural convection in a detailed analysis. Hence the total convective heat loss on both sides of a hot flat plate is given by equation 5 [28].

$$\dot{Q}_{conv_1} = A_b(h_{top} + h_{bot})(T_b - T_{air}) \tag{5}$$

The natural convective heat transfer coefficients at the top and bottom can be calculated using equations 6 and 7 [23,24]. The Grashof (Gr) and Prandtl (Pr) numbers can be defined by equations 8 and 9.

$$h_{top} = [0.27(Gr\mathrm{Pr})^{0.33}]\frac{k_b}{L} \tag{6}$$

$$h_{bot} = [0.14(Gr\mathrm{Pr})^{0.25}]\frac{k_b}{L} \tag{7}$$

$$Gr = \frac{g\beta\rho^2\left(T_a - T_{b_i}\right)L^2}{\mu} \tag{8}$$

$$Pr = \frac{c_b\mu}{k} \tag{9}$$

Regarding equations 6 and 7, the convection heat transfer coefficient at the top surface is larger than at the bottom surface because of the effects of buoyancy [29]. Substituting equation 6 and 7 in 5 will result in the following equation:

$$\dot{Q}_{conv_1} = \frac{k_b}{L} A_b[0.27(GrPr)^{0.33} + 0.14(GrPr)^{0.25}](T_b - T_{air}) \tag{10}$$

The radiative heat transfer from the blank Q_{rad} to the surrounding floor and ceiling surfaces in the plant can be expressed by equation 11 [28]. Regarding equation 11, a shape factor of unity has been applied.

$$\dot{Q}_{rad} = \sigma\varepsilon A_b(T_b^4 - T_{fac}^4) \tag{11}$$

It has been mentioned earlier that the blank loses heat on both sides as shown on figure 1. Thus the heat lost in equation 11 is doubled as shown in equation 12.

$$\dot{Q}_{rad_1} = 2\sigma\varepsilon A_b(T_b^4 - T_{fac}^4) \tag{12}$$

A single equation for the transfer phase can then be formulated based on equation 3. This equation is obtained by substituting equation 10 and 12 into equation 3 as shown below.

$$\dot{Q}_{tran} = \frac{k_b}{L} A_b[0.27(GrPr)^{0.33} + 0.14(GrPr)^{0.25}](T_b - T_{air}) + 2\sigma\varepsilon A_b(T_b^4 - T_{fac}^4) \tag{13}$$

2.2 Placement Stage

The placement phase is the time that the blank is brought between the punch and the die before forming takes place as shown in figure 3.

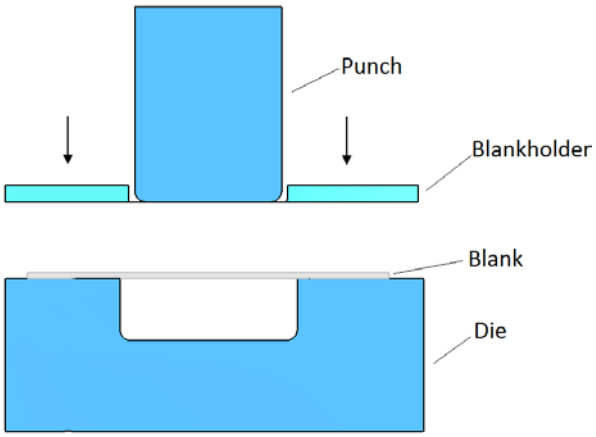

Figure 3 Hot stamping placement phase

During the placement phase, the top surface of the blank is cooled by natural convection through ambient air and radiation exchange with the punch and blank holder. The bottom surface can be split into three sections. Two of the sections are cooled by thermal contact with the die surface. To effectively cool the blank, cooling channels are inserted in the die and punch. Hence the punch and die are assumed to be at a lower temperature than the blank. The other blank section on top of the die cavity is cooled by natural convection with air and radiation exchange with the die [7]. This can be expressed using equation 14.

$$\dot{Q}_{plac} = (\dot{Q}_{conv_2} + \dot{Q}_{rad_2}) + (\dot{Q}_{con_1} + \dot{Q}_{conv_3} + \dot{Q}_{rad_3}) \tag{14}$$

The heat lost by natural convection with ambient air at the upper side of blank can be expressed using equation 15 [28].

$$\dot{Q}_{conv_2} = Ah_{top}(T_b - T_{air}) \tag{15}$$

It is assumed that the punch and blank holder are at the same initial temperature. Hence the radiative heat transfer from the blank to the punch and blank holder can be expressed using the usual radiation heat transfer expression shown in equation 16 [29]. The radiation shape factor f_1 between the upper surface area of the blank and the lower surface area of the punch and blank holder is considered. The surface area of the blank, which is exposed to the punch and blank holder A_{bp} is also considered.

$$\dot{Q}_{rad_2} = \sigma\varepsilon A_{bp} f_1(T_b^4 - T_p^4) \tag{16}$$

The IHTC at the interface between the blank and the die during placement R_{plac} is affected by the surface area, lubrication conditions and integrity of the contacting surfaces [20]. Figure 4 shows that heat transfer occurs at certain points and this reduces the overall contact area thus affecting the IHTC.

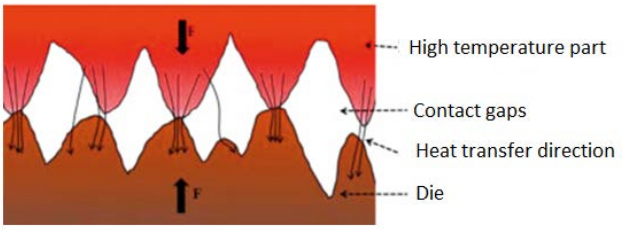

Figure 4 Surface topography at the blank and die interface [20]

Equation 17 shows the heat transfer at the interface between blank and die. The surface area of the blank in contact with the die A_{bd_1} is again considered.

$$\dot{Q}_{con_1} = R_{plac} A_{bd_1} (T_b - T_d) \quad (15)$$

The heat loss by natural convection between the blank and the air space in the die cavity can again be expressed by equation 18.

$$\dot{Q}_{conv_3} = h_{bot_2} A_{bd_2} (T_b - T_{air}) \quad (16)$$

It must be noted that the position of the blank on the die might limit the amount of convection heat transfer depending on the process set up.

Equation 19 shows the radiative heat transfer between the blank and the cavity. The net radiation shape factor f_2 between the bottom and sides of the cavity and the bottom of the blank is considered. The quantity A_{bd_2} represents the surface area of the blank under the die cavity.

$$\dot{Q}_{rad_3} = \sigma \varepsilon A_{bd_2} f_2 (T_b^4 - T_d^4) \quad (17)$$

The total heat lost by the blank during the approach phase can be expressed using equation 20, which is obtained by substituting equation 15, 16, 17, 18 and 19 into equation 14.

$$\dot{Q}_{plac} = \left[A h_{top} (T_b - T_{air}) + \sigma \varepsilon A_{bp} f_1 (T_b^4 - T_p^4)\right] + \left[R_{plac} A_{bd_1} (T_b - T_d) + h_{bot_2} A_{db_2} (T_b - T_{air}) + \sigma \varepsilon A_{bd_2} f_2 (T_b^4 - T_d^4)\right] \quad (18)$$

2.3 Forming and Quenching Stage

It is assumed that forming and quenching occur simultaneously. During the forming and quenching stage, contact heat transfer occurs between the hot blank and cold tool. Figure 5 shows the interfaces during forming and quenching. The deformation of the blank into the die cavity causes sliding contact with the blank holder. However, heat conduction to the blank holder during the forming stage has been assumed to be negligible because of the small sliding time of the blank (0.92 s) [7] and relative low contact pressure.

It is also assumed that the heat lost to the environment is negligible since the temperatures of the punch and die are controlled by the cooling fluid over time. After the forming stage, the blank is held in the closed tool to allow cooling for about 15 to 25 s [11].

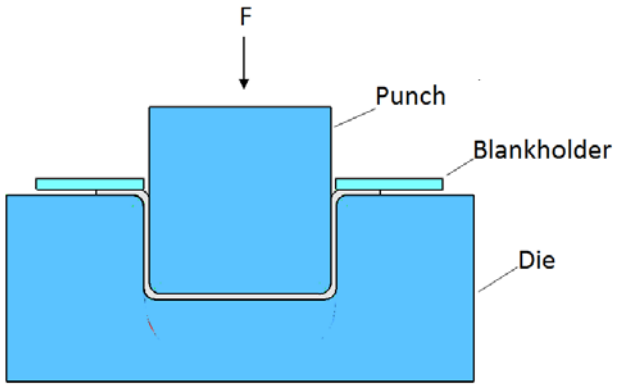

Figure 5 Interfaces during forming and quenching

2.3.1 General considerations

The following work rates and heat transfer scenarios have been considered for the forming and quenching phases:

- Heat absorbed by the punch from the blank surface ($\dot{Q}_1$)
- Heat absorbed by the die from the alternate blank surface ($\dot{Q}_2$)
- Heat transferred from the die surface to the internal die cooling channel walls ($\dot{Q}_3$)
- Heat transfer from the internal die cooling channel walls to the coolant ($\dot{Q}_4$)
- Heat carried by the coolant in the die cooling channels ($\dot{Q}_5$)
- Rate of work done on the blank as a results of frictional forces ($\dot{W}_1$)
- Rate of work done on the blank due to plastic deformation ($\dot{W}_2$)
- Heat released in the blank due to metallurgical transformations (assuming exothermic) ($\dot{Q}_6$)

The blank changes in temperature as a result of heat arising from the work done due to frictional forces ($\dot{W}_1$), plastic deformation ($\dot{W}_2$), heat released during metallurgical transformation ($\dot{Q}_6$), heat absorbed by the die ($\dot{Q}_2$) and the punch ($\dot{Q}_1$). Hence the sum of heat transfer and work rates during forming can be expressed as shown in equation 21.

$$\dot{Q}_{form} = (\dot{Q}_1 + \dot{Q}_2) - (\dot{W}_1 + \dot{W}_2 + \dot{Q}_6) \quad (19)$$

The amount of heat transferred from blank to the tool depends on the design of the tool, surface area and geometry of the blank for a specific part. For simplicity we ignore any transient thermal differences between both water cooled punch and die. Therefore, the following discussion focuses on die only. Transients within the die are accounted for through the IHTC discussed below. As mentioned earlier, the heat lost by the tool to the environment is assumed negligible. Hence, it follows that the heat which is transferred from the die surface to the cooling channel walls $\dot{Q}_3$ is assumed to be equivalent to the heat transferred from the cooling channel walls to the coolant $\dot{Q}_4$ and the heat carried by the moving coolant $\dot{Q}_5$ [9,30] as shown in equation 22. However, this might depend on the set up of a given process.

$$\dot{Q}_1 = \dot{Q}_2 = \dot{Q}_3 = \dot{Q}_4 = \dot{Q}_5 \quad (20)$$

The following section discusses the heat transfer scenarios during the forming and quenching phase.

2.3.1.1 Interface heat transfer from blank surface to the die surface

Heat is transferred from the blank surface to the punch/die surface upon contact. It is assumed that the punch and die are kept at the same temperature and that heat is evenly distributed between them. The heat transfer from the blank surface to the die surface is defined by equation 23 [16].

$$\dot{Q}_2 = R_{form} A_b (T_b - T_d) \quad (21)$$

In order to analyse the heat transfer during the forming and quenching phases, it is necessary to determine the IHTC between the blank and die/punch [19]. The IHTC is an important parameter since it determines the forming and quenching time [16]. The IHTC is also required in order to perform an accurate Finite Element analysis of the hot stamping process [26]. Furthermore, it can be utilized to determine the effect of other process parameters (pressure, temperature and surface roughness) on heat transferability. Therefore, the following section gives an overview and analysis of the methods that have been developed to determine the IHTC between the die/punch and blank.

2.3.1.2 Inverse heat conduction analysis

One of the methods that have been utilized involves using inverse heat conduction analysis to obtain heat flux between blank and die and using it to calculate the IHTC [17,19,31,32]. The method is based on equation 24 [31].

$$\frac{\dot{Q}}{A} = R_{form}(T_{b(t)} - T_{d(t)}) \quad (22)$$

The temperature values $T_{b(t)}$ and $T_{d(t)}$ and the heat flux $(\frac{\dot{Q}}{A})$ are pre-determined to obtain the IHTC. The heat flux is obtained by using Fourier's law of conduction as shown in equation 25 [17].

$$\frac{\dot{Q}}{A} = -k_{b,d} \frac{dT_{b,d}}{dx} \quad (23)$$

The limitation of the method is that it is a challenge to measure the temperature of the blank and die during the forming and quenching operation. Bai *et al*. [31] developed a numerical procedure for determining temperature at specific locations on a work piece and die in a turbine blade forging process. Physical measurements were also done with thermocouples at the specified locations. The heat flux was then computed to obtain the IHTC (3.5 kW/m^2 K). To validate the developed procedure, the calculated IHTC was used in a Finite Element model with conditions similar to the experiment. The results showed that the temperature values obtained from the FE simulation were very close to the numerical procedure. Kim *et al*. [18] used the inverse heat analysis technique to develop a model for the IHTC as a power function of contact pressure, which was evaluated using Finite Element analysis. The model was tested for predicting the phase transformation of a blank in hot stamping. According to the results, a martensitic phase ratio of 87 % was obtained from the experiments and 84 % was obtained from the Finite Element Analysis. Li *et al*. [19] developed software for calculating the IHTC between a hot stamping die and blank using the inverse heat conduction analysis. The software was used to determine the effect of die surface temperature and contact pressure on the IHTC. According to the results, the IHTC (W/m^{2}K) for different pressure values of 1, 10, 20 and 40 MPa led to the derivation of a linear function. The surface temperature of the blank was found not to have a significant effect on the IHTC [19].

2.3.1.3 Newton's law of cooling

Newton's law of cooling can be used to determine the IHTC [16,22,33,34,35]. This method is based on equation 26.

$$T_{b(t)} = (T_{bo} - T_{di}) e^{\frac{-R_{form} A_b t}{\rho V c_b}} + T_{di} \quad (24)$$

Making R_{form} the subject of the equation results in equation 27 [34].

$$R_{form} = \frac{-\rho V c_b}{A_b t} ln \left[\frac{T_{b(t)} - T_{di}}{T_{bo} - T_{di}}\right] \quad (25)$$

Other parameters in the equation can then be identified and used for the calculation of the IHTC. The temperature values can be measured through the use of integrated thermocouples in the blank and die [36]. Merklein *et al*. [33] studied the thermal behaviour of tailored blanks by analysing the effect of a constant IHTC on different tool temperature (between 20 and 300 K), pressure and gap between blank and die. In the study, Newton's law of cooling was used in calculating the IHTC and heated cartridges were used to control the die temperature. However, the challenge of assuming constant surrounding temperature was a limitation on the model since the heat transferred by the blank to the tool results in a change of tool temperature. Hung *et al*. [36] used Newton's law of cooling to investigate the effect of the contact pressure on the IHTC during hot stamping. A Finite Element analysis model was also developed using ABAQUS [16] to evaluate the results. According to the results, IHTC increased from 1764 to 3782 W/m^{2}K with an increase in pressure from 0 to 30 MPa. However, comparing the two models, the FE model gave more accurate results and it proved that the IHTC changed with time unlike Newton's law of cooling, which gave one constant value. Bosetti *et al*. [34] also carried out a similar study to investigate the effect of contact pressure on the IHTC under conditions similar to industry. Two approaches were used, namely Newton's law of cooling and the inverse heat conduction analysis. Both approaches showed that the contact pressure directly affects IHTC. However, the challenge with the study lies on the great deviation between the values of IHTC, which were obtained for the same pressure. For example, a contact pressure of 5 MPa resulted in an IHTC of 1000 W/m^2 K using the inverse heat conduction analysis and 1231 W/m^2 K using Newton's law of cooling.

2.3.1.4 Heat balance method

Zhao *et al*. [17] modified the model for Newton's law of cooling to cater for the change in tool temperature and named it the heat balance method. The heat balance method is based on the assumption that all the heat that is lost by the blank is absorbed by the die and punch (energy conservation law). In developing the model, the authors considered the heat transfer to the die only. Equation 28 below can be used to mathematically describe the method [17].

$$c_b \rho V \frac{dT_b}{dt} = -R_{form} A_b (T_b - T_d) \quad (26)$$

Regarding equation 28, the left side represents the change in internal energy of the blank and the right side shows the heat transfer from the blank to the die at the interface. Since the temperature of the tool changes during the forming and quenching processes, equation 28 can be integrated to yield equation 29 below.

$$\int_{T_{bo}}^{T_{bi}} dT_b = -\frac{R_{form}A_b}{c_b\rho V}\int_{t_o}^{t_i}(T_b - T_d)dt \quad (27)$$

Unlike Newton's law of cooling, the tool temperature T_d changes with time. The equation can be solved using the trapezoidal rule as shown in figure 6 since both the punch and die temperature vary linearly with time. When the area under the graph is determined using the trapezoid rule, the equation becomes

$$T_{b_i} - T_{b_i} = -\frac{R_{form}A_b}{c_b\rho V} * \frac{1}{2}[(T_{bo} - T_{do}) + (T_{bi} - T_{di})] * (t_i - t_o) \quad (28)$$

The difference in the time from t_o to t_i becomes the cooling time (t) of the blank.

$$T_{bi} - T_{bo} = -\frac{R_{form}A_b}{2c_b\rho V}[(T_{bo} - T_{do}) + (T_{bi} - T_{di})]t \quad (29)$$

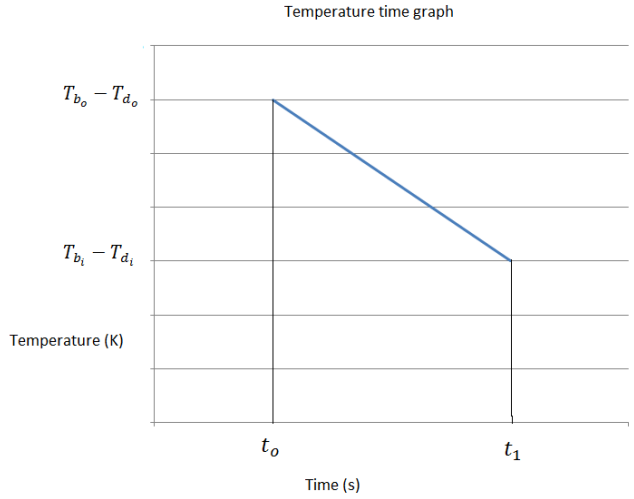

Figure 6 Area under temperature time graph [17]

Rearranging the equation and making R_{form} the subject will result in equation 32. Here, the volume V and the area A are divided to give the characteristic thickness, y, of the blank.

$$R_{form} = \frac{2c_b\rho y(T_{b_o} - T_{b_i})}{\left|(T_{b_i} - T_{d_i}) + (T_{b_o} - T_{d_o})\right|t} \quad (30)$$

Again, it is assumed that half of the heat lost by the blank is transferred to the punch and the other half is transferred to the die. Thus, half the thickness of the blank y is considered as the characteristic thickness. According to Zhao *et al.* [17], experimental analysis shows that equation 29 gives a good prediction of IHTC at the start and end of the quenching process. However, it did not yield an accurate IHTC during the phase transformation. In the study, Zhao *et al.* [17] compared the accuracy of the inverse heat conduction analysis, heat balance and optimization method. Experimental devices were used to collect data on the surface and inside temperature of the blank and die. The accuracy of the methods was evaluated based on a Finite Element simulation of the experiment. According to the results, the inverse heat conduction analysis had an error of 3.7 %, the heat balance method gave an error of 7.5 % and the optimization method had an error of 10.3 %.Ying *et al.* [37] compared the accuracy of the inverse heat conduction analysis and heat balance method during hot forming of a 7075-T6 Aluminium alloy. Average error rates of 3.08 and 4.4 % were obtained using the inverse heat conduction analysis whilst the heat balance method resulted in 14.79 and 4.48 %. Hence, the inverse heat conduction analysis was found to be more accurate when compared to the heat balance method.

2.3.1.5 Optimization method

Another method involves the use of an optimization procedure and treating the IHTC as a design variable as illustrated by Hu *et al*. [38] and Zhang *et al.* [21]. The main objective of the method is to find the optimum IHTC that will result in simulated temperature values, which are almost similar to measured values recorded using thermocouples at the respective locations on the die. The method involves estimating the IHTC and using it to simulate temperature values at various locations of the tool and blank. The temperatures are also measured at the respective locations using thermocouples. The IHTC will then be readjusted and iterations will be done until there is minimum difference between the measured and simulated temperature recordings. The procedure can be summarized using figure 7.

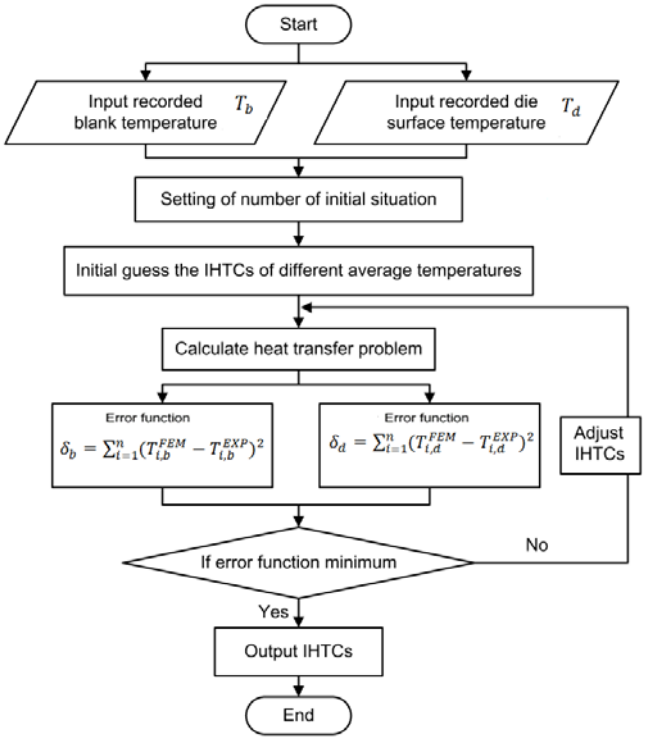

Figure 7 Flow chart for the FEM optimization procedure [38]

Regarding figure 7, the quantities $T_{i,b}^{EXP}$ and $T_{i,b}^{FEM}$ represent the temperature values of the blank recorded by thermocouples and those calculated by the FEM model. The tool temperature readings from the thermocouples and model are represented by the symbols $T_{i,d}^{EXP}$ and $T_{i,d}^{FEM}$. The quantity δ represents the error function which must be minimized for the optimum IHTC [2]. The challenge with using the method is that it results in an average constant IHTC as revealed by Wendelstorf *et al.* [39] and Zhao *et al.* [17].

This might not give an accurate picture of the process since the IHTC is subject to change during the forming and quenching process. Another challenge with the method is that there is a need for separate software to perform the optimization procedure. It is also a tiresome and extensive exercise to perform the iterations in order to obtain the optimum value. Hu *et al*. [38] used the method to determine the effect of IHTC on the oxide thickness (9 to 15 µm) and contact pressure (8 to 42 MPa). The IHTC decreased with an increase in oxide layer thickness. The average IHTC also increased from 2502 W/m^{2}K to 5122 W/m^{2}K as the pressure increased from 8 to 42 MPa. The limitation of the study is that challenges were faced in obtaining accurate readings at high temperatures due to the instability of the mechanical system in the experiments. Similar work was done by Zhang *et al*. [21] to determine the effect of IHTC on the contact pressure. The results did not show a linear relationship between the IHTC and the contact pressure as mentioned by other authors in literature [19,33,34,38]. This could have been caused by the measurement errors in the experiments.

2.3.1.6 Experimental methods

Research efforts have also been done to develop equipment for measuring the IHTC. For example, Ji *et al*. [16] developed equipment for testing the IHTC in the hot stamping of an aluminium alloy (AA5754) according to equation 24. The equipment was integrated with a thermo-mechanical simulator and a control system for temperature and pressure. The effect of pressure on the IHTC was studied and a Finite Element model developed using ABAQUS [16] was implemented to simulate the experiment. Both the model and tests gave the similar values of IHTC. According to the results, the IHTC increased with an increase in pressure until a maximum value was reached which could not increase for pressure above 100 MPa. On the other hand, it should be noted that typical industrial hot stamping processes normally use pressure below 50 MPa.

Studies have shown that the surface roughness and presence of an oxide layer affect the IHTC [20,38,40]. Caron *et al*. [26] developed a model to relate surface roughness and IHTC according to equation 33.

$$R_{form} = \Phi_s + \Phi_g \tag{31}$$

The quantities Φ_s and Φ_g represent the solid conductance and air gap conductance and can be defined by equation 34 and 35 respectively [26].

$$\Phi_s = 1.45 k_{av} \frac{|\tan(s)|}{\eta} \left(\frac{P}{H}\right)^{0.985} \tag{32}$$

$$\Phi_g = \frac{k_{air}}{g} \tag{33}$$

The model was used to calculate the IHTC in hot stamping and experiments were conducted based on the inverse conduction analysis to validate the model. According to the results, the IHTC range obtained using a pressure of 3.2 MPa at the die and blank interface was 10.8 to 19.4 kW/m^{2}K and the range at the punch and blank interface was 8.8 to 16.8 kW/m^2 K. This is far from the value (6.94 kW/m^{2}K) which was obtained using the model in equation 33. Results obtained by other authors are also in contrast with the IHTC value obtained from the model at the same contact pressure [33,34]. Thus there is need for more studies in establishing an accurate co-relation between pressure and IHTC.

2.3.2 Heat transfer from the die surface to the cooling channel wall

The heat transferred from the die surface to the cooling channel walls can be illustrated using figure 8.

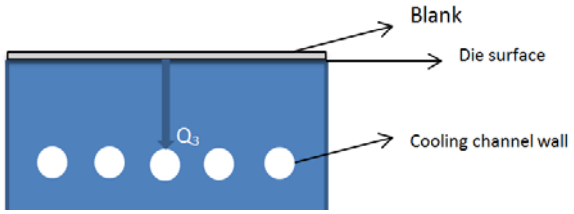

Figure 8 Heat transfer from die surface

To determine the amount of heat transferred, the conduction shape factor analysis can be used [28]. This is shown in equation 36.

$$\dot{Q}_3 = k_d f_3 (T_d - T_{cw}) \tag{34}$$

Assuming that the die is flat, the shape factor f_3 can be defined by equation 37 [28].

$$f_3 = \frac{2\pi l}{ln\left[\left(\frac{2w}{\pi d}\right)\sinh_w\left(\frac{2\pi Zb}{w}\right)\right]} \tag{35}$$

Substitution equation 37 into equation 36 will give

$$\dot{Q}_3 = k_d \frac{2\pi l}{ln\left[\left(\frac{2w}{\pi d}\right)sinh_w\left(\frac{2\pi Zb}{w}\right)\right]} (T_d - T_{cw}) \tag{36}$$

For a given number of cooling channels n, the total heat transferred from the die surface to the cooling channels becomes

$$\dot{Q}_3 = nk_d \frac{2\pi l}{ln\left[\left(\frac{2w}{\pi d}\right)sinh_w\left(\frac{2\pi Zb}{w}\right)\right]} (T_d - T_{cw}) \tag{37}$$

To increase the heat transfer between the die surface and the cooling channel wall, the number of cooling channels can be increased. Another way is to improve the design of cooling channels so as to increase the value of f_3. On the other hand, using tool materials with improved thermal conductivity also helps to increase heat transfer [3].

2.3.3 Heat transfer from the cooling channel walls to the coolant

Equation 40 can be used to determine the heat lost from the cooling channel wall to the coolant.

$$\dot{Q}_4 = h_w A_{cw} (T_{cw} - T_w) \tag{38}$$

The surface area of the channels A_{cw} can be defined by equation 41.

$$A_{cw} = \pi d l \tag{39}$$

The convection heat transfer coefficient can be obtained using Nusselt number as shown in equation 42.

$$h_w = \frac{Nuk_w}{d} \tag{40}$$

If equation 41 and 42 are substituted into equation 40, the total heat transfer from cooling channel walls to the coolant for a given number of cooling channels n becomes

$$\dot{Q}_4 = nNuk_w \pi l (T_{cw} - T_w) \tag{41}$$

To improve the heat transfer between the cooling channel walls and the coolant, the diameter of the cooling channels

and coolant velocity can be increased to rise the value for *Nu*. However, the effect of the yield stress of the material must be taken into consideration to prevent tool deformation.

2.3.4 Heat carried by the coolant in the channels

The heat removal rate by the water in the cooling channels is defined by equation 44 [41].

$$\dot{Q}_5 = \dot{m}c_w(T_{out} - T_{in}) \quad (42)$$

2.3.5 Heat balance between tool surface and coolant

Equation 45 has been proposed for the energy balance during the forming and quenching stage. Equation 45 is obtained by substituting equation 39, 43 and 44 into equation 22. This is based on the assumptions made in equation 22.

$$nk_d \frac{2\pi l}{ln\left[\left(\frac{2w}{\pi d}\right)sinh_w\left(\frac{2\pi Zb}{w}\right)\right]}(T_d - T_{cw}) = nNuk_w\pi l(T_C - T_w) = \dot{Q}_5 = \dot{m}c_w(T_{out} - T_{in}) \quad (43)$$

2.3.6 Rate of work done due to friction and plastic deformation

The rate of work done due to friction depends on the normal contact force (F_1) and the sliding speed (v_1) as shown in equation 46 [42].

$$\dot{W}_1 = \mathfrak{n}F_1v_1 \quad (44)$$

Equation 47 describes the rate of work done during plastic deformation [43,44].

$$\dot{W}_2 = \lambda V \int_0^{\epsilon} \tau \, d\epsilon \quad (45)$$

Regarding equation 47, the Taylor Quinny- coefficient λ is the fraction of plastic work which is converted into heat [45]. The heat generated due to plastic work acts to thermally soften the material.

2.3.7 Heat released due to metallurgical transformations

The martensitic transformation of the blank results in release of latent heat which can be expressed using equation 48 below [35,44].

$$\dot{Q}_6 = mEU/t \quad (46)$$

The fraction for martensitic transformation *U* is given by the Koistinen-Marbuger law as shown in equation 49, where α represents the stress dependent transformation constant and T_{ms} is the martensitic start temperature [35].

$$U = 1 - e^{-\alpha(T_{ms} - T_b)} \quad (47)$$

Substituting equation 49 into 48 results in

$$\dot{Q}_6 = mE\left(1 - e^{-\alpha(T_{ms} - T_b)}\right)/t \quad (50)$$

For a typical 22MnB5 steel, the values of *E* (latent heat), α and T_{ms} are 85 kJ/kg, 3.02577 K^{-1} and 411.3 K respectively [35].

2.3.8 Equation for heat transfer during forming

The equation for the forming stage can be obtained by substituting equations 36, 46, 47 and 50 into 22 as shown in equation 51. The heat transfer in equation 23 is doubled to include the heat transferred to the punch. This is based on the above assumption that the punch and die absorb heat in equal shares during the forming and quenching phases ($\dot{Q}_1 = \dot{Q}_2$).

$$\dot{Q}_{form} = 2R_{form}A_b(T_b - T_d) - \left[\mathfrak{n}F_1v_1 + mE\left(1 - e^{-\alpha(T_{ms} - T_b)}\right)/t + \lambda V \int_0^{\epsilon} \tau d\,\epsilon\right] \quad (48)$$

3 Discussion

During the transfer stage, the heat loss of the blank is mainly dependent on the surface area of the blank and the method in which it is transferred from the furnace to the forming tool. Depending on the process set up, it may be necessary to consider forced convection. Regarding the placement stage, the tool geometry and press speed are of great importance. For the forming stage, the surface area, roughness, material properties and temperature of the contacting surfaces have a great influence on heat transfer.

Some of the models for determining IHTC use direct temperature measurements. The challenge with such a practice is that it is difficult to obtain accurate readings from the thermocouples since the temperatures change rapidly and the response time of the thermocouples needs to be considered. The thermocouples are also exposed to high pressure conditions and this can also have a negative effect on the resultant readings. On the other hand, use of FEM requires the input of several process parameters and there are also a lot of iterations involved. Literature analysis has revealed that the inverse heat conduction analysis is the most accurate method and the FEM based method is the least accurate method for calculating IHTC. Based on the analysis made, equation 52 is proposed for the overall heat transfer. It is obtained by substituting equation 13, 20 and 51 into equation 2.

$$\dot{Q}_{total} = -\left[\frac{k_b}{L}A_b[0.27(GrPr)^{0.33} + 0.14(GrPr)^{0.25}](T_b - T_{air}) + 2\sigma\varepsilon A_b(T_b^4 - T_{fac}^4)\right] - \left[\left(Ah_{top}(T_b - T_{air}) + \sigma\varepsilon A_{bp}f_1(T_b^4 - T_p^4)\right) + R_{plac}A_{bd_1}(T_b - T_d) + h_{bot_2}A_{db_2}(T_b - T_{air}) + \sigma\varepsilon A_{bd_2}f_2(T_b^4 - T_d^4)\right] - \left[2R_{form}A_b(T_b - T_d) - \left(\mathfrak{n}F_1v_1 + mE\left(1 - e^{-\alpha(T_{ms} - T_b)}\right)/t + \lambda V \int_0^{\epsilon} \tau \, d\epsilon\right)\right] \quad (49)$$

The proposed equation is useful in identifying the critical parameters, which can be utilized for effective thermal management of the hot stamping process. Effective thermal management in hot stamping is necessary for reducing the cooling time of the blank, which results in a reduction in cycle time thus ultimately leading to productivity improvement and production cost reduction.

4 Conclusion

The aim of the paper was to present a basis for the heat transfer model during the hot stamping process. A comprehensive model governing heat transfer during the hot stamping process was proposed. This is based on the equation developed for the separate process stages. A review on the models for determining IHTC was presented. The next phase of the research involves validation of the proposed model. This can be achieved by conducting experiments and simulation of the hot stamping process. To gain more understanding on the heat transfer during the quenching stage, there is need for further study on the cooling system design. It is necessary to examine the effect of the cooling system parameters on the heat transfer.

References

1. *Liu HS, Xing ZW, Bao J and Song BY,* Investigation of the Hot-stamping Process for Advanced High-strength Steel Sheet by Numerical Simulation, *Journal of Materials Engineering and Performance*, 2010, 19(3), 325-334
2. *Hu P, He B and Ying L,* Numerical Investigation on Cooling Performance of Hot Stamping Tool with Various Channel Designs, *Applied Thermal Engineering*, 2016, 96, 338-351.
3. *Karbasian H and Tekkaya AE,* A Review on Hot Stamping, *Journal of Material Processing Technology*, 2010, 210(15), 2103-2118.
4. *Kolleck R, Veit R, Merklein M, Lechler J and Geiger M.* Investigation on Induction Heating for Hot Stamping of Boron Alloyed Steels, *CIRP Annals - Manufacturing Technology*, 2009, 58(1), 275-278.
5. *Mueller B, Hund R and Malek R,* Added Value in Tooling for Sheet Metal Forming through Additive Manufacturing, *In Proceedings of the International Conference on Competitive Manufacturing (COMA`13)*, Stellenbosch, South Africa, 2013, 51-58.
6. *Liu H, Lei C and Xing Z,* Cooling System of Hot Stamping of Quenchable Steel BR1500HS: Optimization and Manufacturing Methods, *International Journal of Advanced Manufacturing Technology*, 2013, 69(1-4), 211-223.
7. *Abdulhay B, Bourouga B and Dessain C,* Experimental and Theoretical Study of Thermal Aspects of the Hot Stamping Process, *Applied Thermal Engineering*, 2011, 31(5), 674-685.
8. *Ojha S, Mishra NS and Jha BK,* Effect of Cooling Rate on the Microstructure and Mechanical Properties of a C–Mn–Cr–B Steel, *Bulletin of Material Science*, 2015, 38(2), 531-536.
9. *Shan ZD, Zhang ML, Jiang C, Xu Y and Rong WJ,* Basic Study on Die Cooling System of Hot Stamping Process, *Proceedings of the International Conference of Advanced Technology Design Manufacturing*, Beijing, 2010, 65-68.
10. *Lim WS, Choi HS, Ahn SY and Kim BM,* Cooling Channel Design of Hot Stamping Tools for Uniform High-strength Components in Hot Stamping Process, *International Journal of Advanced Manufacturing Technology*, 2014, 70(5-8), 1189-1203.
11. *Steinbeiss H, So H, Michelitsch T and Hoffmann H,* Method for Optimizing the Cooling Design of Hot Stamping Tools, *Production Engineering*, 2007, 1(2), 149-155.
12. *Zamri MF and Yusoff AR,* Heuristic Optimisation of Cooling Channel Design in the Hot Stamping Die for Hot Stamping Process, *Advances in Materials and Processing Technology*, 2015, 1(1-2), 27-35.
13. *Ghiotti A, Bruschi S, Medea F and Hamasaiid A,* Tribological Behavior of High Thermal Conductivity Steels for Hot Stamping Tools, *Tribology International*, 2016, 97, 412-422.
14. *Escher C and Wilzer JJ,* Tool Steels for Hot Stamping of High Strength Automotive Body Parts, *Proceedings of the International Conference of Stone Concrete Machining*, 2015, 3, 219-228.
15. *Altan T and Tekkeya AE,* Sheet Metal Forming Processes and Applications, ASM International, 2012.
16. *Ji K, Fakir OE, Gao H and Wang L,* Determination of Heat Transfer Coefficient for Hot Stamping Process, *Materials Today: Proceedings*, 2015, 2(2), S434 – S439.
17. *Zhao K, Wang B, Chang Y, Tang X and Yan J,* Comparison of the Methods for Calculating the Interfacial Heat Transfer Coefficient in Hot Stamping, *Applied Thermal Engineering*, 2015, 79, 17-26.
18. *Kim H-K, Lee SH and Choi H,* Evaluation of Contact Heat Transfer Coefficient and Phase Transformation during Hot Stamping of a Hat-type Part, *Materials*, 2015, 8(4), 2030-2042.
19. *Li H, He L, Zhang C and Cui H,* Research on the Effect of Boundary Pressure on the Boundary Heat Transfer Coefficients between Hot Stamping Die and Boron Steel, *International Journal of Heat and Mass Transfer*, 2015, 91, 401-415.
20. *Chang Y, Tang X, Zhao K, Hu P and Wu Y,* Investigation of the Factors Influencing the Interfacial Heat Transfer Coefficient in Hot Stamping, *Journal of Material Processing Technology*, 2016, 228, 25-33.
21. *Zhang Z, Gao P, Liu C and Li X,* Experimental and Simulation Study for Heat Transfer Coefficient in Hot Stamping of High-strength Boron Steel, *Metallurgical and Materials Transactions B*, 2015, 46(6), 2419-2422.
22. *Hung T-H, Tsai P-W, Chen F-K, Huang T-B and Liu W-L,* Measurement of Heat Transfer Coefficient of Boron Steel in Hot Stamping, *Procedia Engineering*, 2014, 81, 1750-1755.
23. Shapiro AB. Using LS-Dyna for Hot Stamping, *Proceedings of the 7th European LS-DYNA Users Conference*, Salzburg, Austria, 2009.
24. *Liu H, Liu W, Bao J, Xing Z, Song B and Lei C,* Numerical and Experimental Investigation into Hot Forming of Ultra High Strength Steel Sheet, *Journal of Materials Engineering and Performance*, 2011, 20(1), 1-10.
25. *Nakagawa Y, Maeno T and Mori KI,* Forming and Quenching Behaviours in Hot Stamping of Thin Quenchable Sheets, *MATEC Web of Conferences* January, 2015.
26. *Caron E, Daun KJ and Wells MA,* Experimental Characterization of Heat Transfer Coefficients during Hot Forming Die Quenching of Boron Steel, *Metallurgical and Materials Transactions B*, 2013, 44(2), 332-43.
27. *Abdulhay B, Bourouga B, Dessain C, Brun G and Wilsius J,* Development of Estimation Procedure of Contact Heat Transfer Coefficient at the Part–tool Interface in Hot Stamping Process, *Heat Transfer Engineering*, 2011, 32(6), 497-505.
28. *Hagen K,* Heat Transfer with Applications, Prentice Hall, New Jersey, 1999.
29. *Cengel YA and Ghajar AJ,* Heat and Mass Transfer: Fundamentals & Application, 5th Edition in SI Units, 2015.

30. *Ying X and Zhong-de S,* Design Parameter Investigation of Cooling Systems for UHSS Hot Stamping Dies, *International Journal of Advanced Manufacturing Technology*, 2014, 70(1-4), 257-262.
31. *Bai Q, Lin J, Zhan L, Dean TA, Balint DS and Zhang Z,* An Efficient Closed-form Method for Determining Interfacial Heat Transfer Coefficient in Metal Forming, *International Journal of Machine Tools Manufacture*. 2012, 56, 102-110.
32. *Caron EJ, Daun KJ and Wells MA.* Experimental heat transfer coefficient measurements during hot forming die quenching of boron steel at high temperatures. *International Journal of Heat and Mass Transf*er 2014, 71, 396-404.
33. *Merklein M, Lechler J and Stoehr T,* Investigations on the Thermal Behavior of Ultra High Strength Boron Manganese Steels within Hot Stamping, *International Journal of Material Forming*, 2009, 2(1), 259-262.
34. *Bosetti P, Bruschi S, Stoehr T, Lechler J and Merklein M,* Interlaboratory Comparison for Heat Transfer Coefficient Identification in Hot Stamping of High Strength Steels, *International Journal of Materials Forming.* 2010, 3, 817-820.
35. *Gu Z-W, Lv M-M, Lu G-H, Xu H and Li X*, Heat Transfer Coefficient Evolution of Boron Steel during Hot Forming Die Quenching, *Material Science and Technology*, 2016, 32(2), 173-180.
36. *Huang R, Riddle M, Graziano D, Warren J, Das S, Nimbalkar S, Cresko J and Masanet E,* Energy and Emissions Saving Potential of Additive Manufacturing: The Case of Lightweight Aircraft Components, *Journal of Cleaner Production*, 2016, 135, 1559-1570.
37. *Ying L, Gao T, Dai M and Hu P,* Investigation of Interfacial Heat Transfer Mechanism for 7075-T6 Aluminum Alloy in HFQ Hot Forming Process, *Applied Thermal Engineering*, 2017, 118, 266-282.
38. *Hu P, Ying L, Li Y and Liao Z,* Effect of Oxide Scale on Temperature-dependent Interfacial Heat Transfer in Hot Stamping Process, *Journal of Materials Processing Technology*, 2013, 213(9), 1475-1483.
39. *Wendelstorf R, Spitzer K and Wendelstorf J,* Effect of Oxide Layers on Spray Water Cooling Heat Transfer at High Surface Temperatures, *International Journal of Heat and Mass Transfer*, 2008, 51(19), 4892-4901.
40. *Ikeuchi K and Yanagimoto J,* Valuation Method for Effects of Hot Stamping Process Parameters on Product Properties using Hot Forming Simulator, *Journal of Materials Processing Technology*, 2011, 211(8), 1441-1447.
41. *Arpaci VS and Selamet A and Kao S.* Introduction To Heat Transfer, Upper Saddle River, 2000.
42. *Van der Heide E,* Lubricant failure in sheet metal forming, Phd Thesis, University of Twente, 2002.
43. *Kapoor R and Nemat-Nasser S,* Determination of Temperature Rise during High Strain Rate Deformation, *Mechanics of Materials*, 1998, 27(1), 1-12.
44. *Hosford WF and Caddell RM,* Metal Forming*:* Mechanics and Metallurgy, 4th Edition, Cambridge University Press, London, 2011.
45. *Rusinek A and Klepaczko JR,* Experiments on Heat Generated during Plastic Deformation and Stored Energy for TRIP Steels, *Materials Design*, 2009, 30(1), 35-48.

